Langmuir

Article

pubs.acs.org/Langmuir

High-Yielding and Photolabile Approaches to the Covalent Attachment of Biomolecules to Surfaces via Hydrazone Chemistry

Ju Hun Lee,[†] Dylan W. Domaille,[†] Hyunwoo Noh,[†] Taeseok Oh,[†] Chulmin Choi,[‡] Sungho Jin,[‡] and Jennifer N. Cha*[,†]

[†]Department of Chemical and Biological Engineering, University of Colorado, Boulder, 596 UCB, Boulder, Colorado 80303-1904, United States

[‡]Department of Mechanical and Aerospace Engineering, University of California, San Diego, 9500 Gilman Drive, M/C 0411, La Jolla, California 92093-0411, United States

Supporting Information

ABSTRACT: The development of strategies to couple biomolecules covalently to surfaces is necessary for constructing sensing arrays for biological and biomedical applications. One attractive conjugation reaction is hydrazone formation—the reaction of a hydrazine with an aldehyde or ketone—as both hydrazines and aldehydes/ketones are largely bioorthogonal, which makes this particular reaction suitable for conjugating biomolecules to a variety of substrates. We show that the mild reaction conditions afforded by hydrazone conjugation enable the conjugation of DNA and proteins to the substrate surface in significantly higher yields than can be achieved with traditional bioconjugation techniques, such as maleimide chemistry. Next, we designed and synthesized a photocaged aryl ketone that can be conjugated to a surface and photochemically activated to provide a suitable partner for subsequent hydrazone formation between the surface-anchored ketone and DNA- or protein-hydrazines. Finally, we exploit the latent functionality of the photocaged ketone and pattern multiple biomolecules on the same substrate, effectively demonstrating a strategy for designing substrates with well-defined domains of different biomolecules. We expect that this approach can be extended to the production of multiplexed assays by using an appropriate mask with sequential photoexposure and biomolecule conjugation steps.

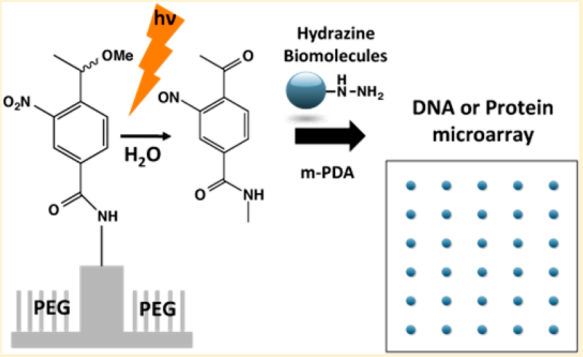

INTRODUCTION

The development of techniques to immobilize biomolecules on micropatterned substrates is necessary to producing biological diagnostics and assays. For instance, DNA microarrays have enabled the measurement of gene expression and allowed researchers to diagnose particular genetic conditions.[1−5] The first DNA microarrays used UV cross-linking or relied on simple electrostatic interactions between DNA and poly-L-lysine-coated glass to monitor gene expression patterns in human cancer or in plants.[2,3] The extension of DNA arrays to patterned protein surfaces has been used to quantify biomolecules in solution, which has helped monitor and study biological processes as well as screen for diseases.[6−18] For protein conjugation to surfaces, Macbeath et al. demonstrated that parallel protein arrays could be produced using Schiff base linkages between aldehyde surfaces and protein amino groups,[7] while Zhu et al. utilized histidine−nickel interactions to anchor proteins to surfaces.[8] In addition, Robinson et al. described a technique to analyze mutiple proteins (autoantibodies) corresponding to eight distinct human autoimmune diseases simultaneously by spotting the antigen microarrays on poly-L-lysine-coated glass.[18] Since these earlier reports, a variety of covalent bioconjugation strategies for producing biomolecule microarrays have been pursued, including the use of active esters,[19] epoxides,[20,21] maleimides,[21] and carbodiimides[22] as well as photochemical cross-linkers.[23−26] These chemistries rely on general nucleophile/electrophile interactions and consequently are limited by lower chemoselectivity and are susceptible to inactivation by water.[7,9,19,22,27,28]

To address these issues, aldehyde-based hydrazone chemistry has been shown to be an excellent reaction for conjugating biomolecules due to its high chemoselectivity and reactivity under mild conditions. The number of reports accelerated after Dirksen et al. reported that the small molecule aniline could catalyze hydrazone and oxime formation and that these conditions were suitable for biomolecule ligation and labeling.[29−35] While hydrazones have previously been used as a surface-patterning chemistry,[9,28] because the hydrazone linkages formed typically arise from the reaction of a hydrazine with an aliphatic aldehyde, these hydrazone linkages are less thermodynamically stable than hydrazone linkages derived from aryl aldehydes.[30,31] As we[36] and others[37] have shown, bis-

Received: February 24, 2014
Revised: June 8, 2014
Published: June 27, 2014

aliphatic hydrazones form exceptionally fast at physiological pH with second-order rate constants on the order of 5−20 M^{-1} s^{-1}, yet the hydrolysis back reaction is also rapid, with first-order rate constants on the order of 10^{-4} s^{-1}. Thus, we sought to pattern surfaces through aryl hydrazone linkages and, based on previous reports,[30] reasoned that the resulting linkage would be more resistant to hydrolysis.

Here, we show that DNA, proteins, and enzymes can be conjugated to aryl aldehyde-derivatized surfaces through hydrazone linkages. The conditions are mild enough that proteins retain their native conformation, as evidenced by the persistence of antibody−antigen interactions, and enzymes retain their enzymatic activity. Next, we designed and synthesized a photocaged ketone compound that rapidly converts to a reactive carbonyl compound in the presence of light and can react with hydrazine nucleophiles under organocatalysis conditions to form stable hydrazone linkages between the surface and biomolecule. Finally, we demonstrate that this approach enables the patterning of multiple biomolecules on the same substrate in photolitographically defined regions.

RESULTS AND DISCUSSION

Photoresist-capped micrometer-sized silicon pillars were produced by lithography and a negative tone photoresist (PR). After the hydroxylation of the non-PR-coated silicon surfaces with nitric acid, the Si regions were passivated with methoxypolyethylene glycol trimethylsilyl ether (PEG-silane) (MW 5000) to minimize nonspecific biomolecule adsorption.[10,38] The substrates were briefly washed with fresh toluene and sonicated in acetone to remove the negative PR from the tops of the Si pillars; these regions were then reacted with 3-aminopropyltriethoxysilane (APTES) to install amine groups on top of the Si pillars (Figure 1a).

We first sought to demonstrate the utility of using an aryl aldehyde to conjugate biomolecules to the surface. To this end, the amine-modified pillars were reacted with 4-formyl succinimidyl benzoate to install aryl aldehyde moieties on the pillar surfaces. The aldehyde density was approximated by conjugating fluorescein hydrazide to the aldehydes, washing away the excess dye, releasing the conjugated dye with pH 4.8 buffer, and measuring the concentration of liberated dye by UV−visible spectroscopy. On the basis of this analysis, we determined that the density of aldehyde groups on the Si pillars was ∼6.4 nmol/cm^2. With the aldehyde-functionalized substrates in hand, we next sought to compare the efficiency of hydrazone-mediated conjugation to traditional bioconjugation methodologies. To this end, the aldehyde substrates were reacted with fluorescein-tagged DNA displaying a 5′-acyl hydrazine (10 μM). We observed high conjugation of the DNA-fluorescein to the aldehyde-functionalized pillars as visualized by fluorescence microscopy and densitometric analysis (Figure 1). As a mode of comparison, DNA microarrays were produced by installing maleimide groups on the Si pillars with succinimidyl-4-(*N*-maleimidomethyl)-cyclohexane-1-carboxylate (SMCC) and then reacting these substrates with fluorescein-tagged DNA displaying a 5′-thiol group. Under these conditions, we observed low conjugation of the DNA to the pillars, indicating that the hydrazone conjugation proceeded more smoothly and efficiently than this standard bioconjugation approach. Indeed, densitometric analysis indicated that the hydrazone-mediated conjugation resulted in 12.5-fold-higher DNA conjugation than the

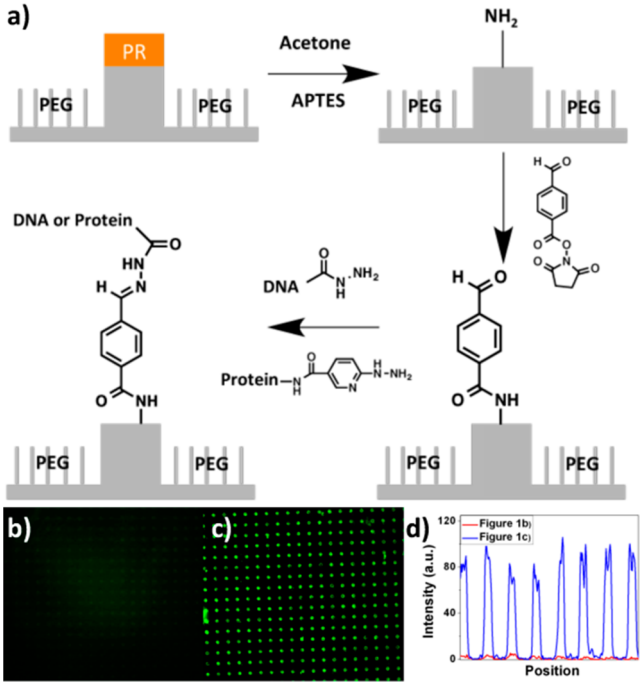

Figure 1. (a) Schematic showing methods used to fabricate the PEG-passivated aldehyde surface and conjugate biomoleulces via hydrazone chemistry. (b) Fluorescent image of maleimide-functionalized substrates reacted with FAM-labeled thiolated DNA. (c) Fluorescent image of aldehyde-functionalized substrates reacted with FAM-labeled hydrazide-DNA. (d) Comparing fluorescence intensity line plots obtained with ImageJ. Red and blue plots corresponded to horizontal fluorescence intensity line profiles of eight representative FAM-DNA immobilized pillars in panel b and c, respectively.

maleimide-thiol chemistry (Figure 1d). It is likely that the high conjugation efficiency of the hydrazone reaction is a result of the high chemoselectivity of the reaction. While aldehyde and hydrazine components selectively react with each other, maleimides can be hydrolyzed by the aqueous buffer conditions, and thiols can oxidize to disulfides, rendering these reagents unreactive in the bioconjugation procedure.

We next explored the potential for attaching proteins through aryl hydrazone chemistry. In this case, fluorescein-labeled antigoat immunoglobulin (IgG) was derivatized with pyridyl hydrazine groups (Materials and Methods). The aldehyde-functionalized Si substrates were reacted with fluorescent hydrazine-derivatized antigoat IgG in 100 mM NH_4OAc buffer at pH 4.8 for 24 h. Again, as a point of comparison, thiolated fluorescent IgG was reacted with maleimide-derivatized Si pillars. While the use of maleimide chemistry yielded a negligible fluorescence signal from fluorescein-labeled IgG (Figure S1a), using hydrazone formation yielded a high amount of bound antibody (Figure S1b). The competitive elution of the fluorescent IgG hydrazine with pH 4.8 buffer and excess hydroxylamine allowed us to estimate that ∼5.76 × 10^8 proteins were conjugated per pillar. Next, we utilized antibody−antigen interactions to investigate whether the hydrazone conjugation procedure would cause protein denaturation. For this, antigoat IgG was derivatized with pyridyl hydrazine groups and anchored to the aldehyde substrate through hydrazone linkages. Next, goat IgG was fluorescently labeled with NHS-fluorescein and incubated with the surface-bound antigoat IgG. As shown in Figure S2, the antigoat IgG microarrays were capable of binding the fluorescein-conjugated

dx.doi.org/10.1021/la500744s | *Langmuir* 2014, 30, 8452−8460

Scheme 1. Synthesis of a Photocaged Ketone Derivative

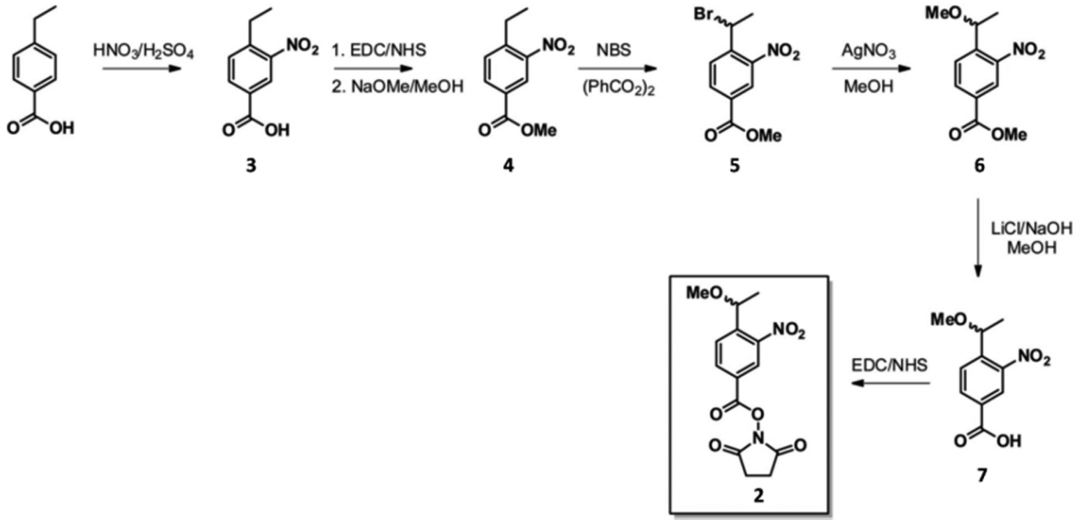

goat IgG; in the absence of conjugated antigoat IgG, no appreciable fluorescein signal was detected. Because antibody–antigen interactions are highly structure-specific, we concluded that conjugating the antigoat IgG with pyridyl hydrazine groups did not cause protein denaturation or activity. To verify this further, we also conjugated the enzyme alkaline phosphatase to the Si pillars using hydrazone chemistry and tested for activity.[39,40] For this, alkaline phosphatase was modified with pyridyl hydrazine groups and conjugated to the aldehyde-functionalized Si substrates. Upon incubation with phosphatase substrate ELF-97, a reagent that forms an insoluble fluorogenic product upon phosphate removal, we saw fluorescent precipitation on the silicon pillars, indicating that the phosphatase activity of the enzyme was retained through the bioconjugation procedure (Figure S3). Taken together, these antibody and enzyme results demonstrate the ability of this conjugation chemistry to pattern proteins on surfaces while preserving the innate biological activity of biomolecules.

With the ability to form stable bioconjugate linkages between surface aldehydes and hydrazine-derivatized biomolecules firmly demonstrated, we next sought to expand this patterning methodology to include photolithography. We reasoned that by using light to uncage a carbonyl that could react with hydrazine nucleophiles, we could integrate this bioconjugation technique with photopatterning to generate a photocontrolled method of patterning DNA, peptides, and proteins on a single surface. In order to achieve this, we first designed a photolabile system that would reveal a hydrazine-reactive carbonyl upon light exposure. For this, we chose to use an *o*-nitrobenzyl alcohol substrate. Typically, this class of compounds is used to photocage an alcohol or carboxylic acid: upon irradiation with UV light, the compound releases the alcohol or carboxylate component with concomitant production of an *o*-nitrosobenzaldehyde.[41−43] Thus, if we could anchor the *o*-nitrobenzyl alcohol substrate to the surface, we could generate a reactive electrophile upon light exposure and use this photogenerated electrophile for subsequent reaction with a hydrazine-derivatized biomolecule.

In our initial experiments, we examined the ability to use an *o*-nitrobenzyl ether to photoconvert to its corresponding *o*-nitrosobenzaldehyde **1**. However, we observed that the photogenerated aldehyde was unstable and rapidly decomposed (Figure S4). This observation is consistent with previous mechanistic investigations of *o*-nitrobenzyl alcohol/ether photoconversions.[42] In order to circumvent the instability of the photochemically revealed aldehyde, we designed a photocaged ketone **2** (Scheme 1). The resulting *o*-nitrosoacetophenone derivative has been reported to be much less susceptible to degradation than the corresponding benzaldehyde derivative.[42] Upon irradiation with UV light, this compound should liberate methanol to generate an acetophenone (ketone) derivative to react with hydrazine-derivatized biomolecules. Initial experiments with acetophenone-modified surfaces confirmed that surface-bound aryl ketones are reactive with hydrazines and allowed us to identify optimal conditions for bioconjugation to these functionalities (Figure S5).

The synthesis of NHS-ester **2** was achieved in six steps from 4-ethyl benzoic acid (Scheme 1, Materials and Methods) with minimal chromatography. The nitration of 4-ethyl benzoic acid in a mixture of H_2SO_4 and HNO_3 installed a nitro group adjacent to the ethyl substituent. After the precipitation of this compound in ice water, **3** was converted to its corresponding activated ester with EDC and *N*-hydroxysuccinimide and then immediately reacted with NaOMe to yield the methyl ester in 79% over two steps. Radical bromination of **4** was carried out with *N*-bromosuccinimide (NBS) and a benzoyl peroxide initiator. After an overnight reaction, benzyl bromide **5** was isolated, and we attempted to displace the bromide with the methoxide ion; however, this approach led to an intractable mixture of products. Thus, a methanolic solution of $AgNO_3$ was used to facilitate the replacement of the bromide with a methoxy group under neutral conditions, which furnished methyl ether **6** in good yield. Next, the methyl ester group was hydrolyzed with NaOH in the presence of LiCl, and the crude material was extracted and precipitated slowly from a concentrated solution of ethyl acetate with petroleum ether. This afforded carboxylic acid **7** as a white solid in high yield (98%) and purity. Finally, **7** was converted to its corresponding NHS-ester in the presence of EDC and *N*-hydroxysuccinimide, providing the final photocaged ketone compound, **2**.

We monitored the photoconversion of compound **7** by ^{1}H NMR to confirm that it would form the expected *o*-nitrosoacetophenone derivative upon exposure to light (Figure S6). A solution of **7** in MeOH/DI water (3:1) was exposed to 15 min of irradiation with a mercury vapor short arc lamp, and

dx.doi.org/10.1021/la500744s | *Langmuir* 2014, 30, 8452−8460

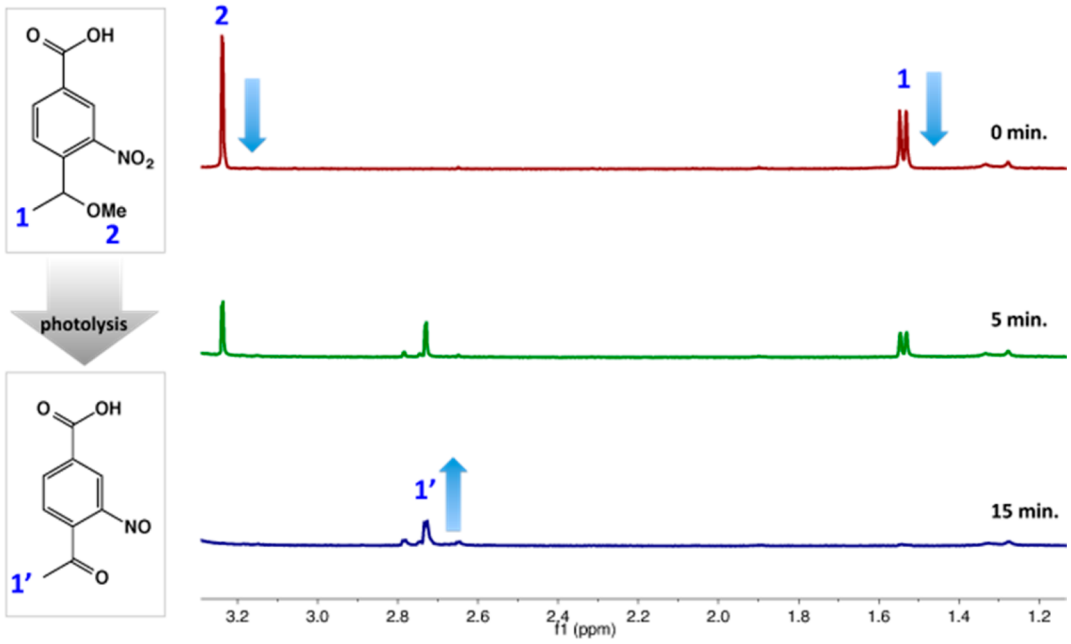

Figure 2. Time-course ^{1}H NMR study for the conversion of the photocaged ketone with various degrees of light exposure. The first spectrum was recorded without light exposure in MeOD/D_2O (3:1), and the second and third spectra were recorded after 5 and 15 min of light exposure, respectively.

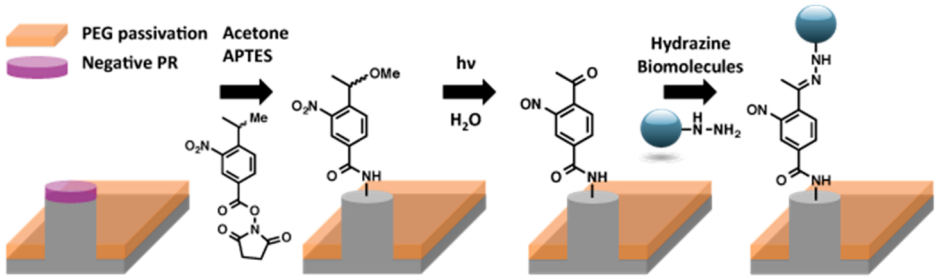

Figure 3. Schematic showing how patterned biomolecules were generated from photocaged ketones. The photoresist was first removed with acetone, and the Si pillars were derivatized with ATPES. Next, amine-functionalized Si pillars were reacted with the NHS ester of the photocaged ketone. Upon photoillumination, ketone groups were exposed, and these could be reacted with hydrazine-derivatized biomolecules.

the progress of the reaction was monitored by ^{1}H NMR; the time-course NMR study is shown in Figure 2. We saw clean photoconversion to the corresponding ketone as evidenced by the disappearance of the benzylic and methoxy group protons and the emergence of a singlet centered at 2.7 ppm, corresponding to the ketone methyl group. In contrast to the photogenerated aldehyde, the photogenerated ketone was stable under these reaction conditions, indicating that this reagent would be suitable for subsequent reaction with a hydrazine-derivatized biomolecule. These data indicated that not only does the photoconversion proceed cleanly without side products but the compound also photolyzes rapidly with complete conversion after only 15 min of light exposure.

The photocaged ketone groups were then installed on the Si pillars by reacting NHS-ester **2** with the amine-derivatized pillars (Figure 3). Next, the substrates were exposed to UV light in pH 5.5 deionized water and MeOH and irradiated with a mercury vapor arc lamp for 30 min, transferred to pH 8.0 phosphate buffer for 10 min, washed, and incubated overnight at pH 4.8 with hydrazide-DNA bearing a fluorescein group. In contrast to our initial expectations, we saw very low conjugation of the DNA to the ketone substrate. We reasoned that the low conjugation efficiency was a result of the lower reactivity of ketones in forming hydrazones. While the ketone derivatives are more stable and form fewer side products during photogeneration, the reaction of an aryl ketone with a hydrazide has slower reaction kinetics than the reaction between an aldehyde and a hydrazide.[44] Thus, we initiated a search for an efficient organocatalyst that would facilitate the formation of the hydrazone between the biomolecule hydrazine and surface ketone.

Aniline is a common small-molecule organocatalyst often used to enhance the rate of hydrazone formation with aldehydes; however, ketones require more efficient catalysts due to their lower reactivities.[45] To increase the rate of hydrazone formation between the photolyzed ketone and hydrazine-functionalized biomolecules, we screened three catalysts that have been reported to catalyze hydrazone formation: aniline, anthranilic acid, and *m*-phenylenediamine (*m*-PDA).[45,46] Ketone-modified pillars were reacted with DNA-hydrazide bearing a fluorescein tag in the presence of 10 mM anthranilic acid or aniline or 150 mM m-PDA in pH 4.5 buffer (Figure 4, Figure S7). We measured the fluorescence intensity of each pillar for each experimental condition and observed that *m*-PDA increased the DNA loading by ∼4.2-fold above that of aniline and 3.0-fold above that of anthranilic acid. Though

dx.doi.org/10.1021/la500744s | *Langmuir* 2014, 30, 8452−8460

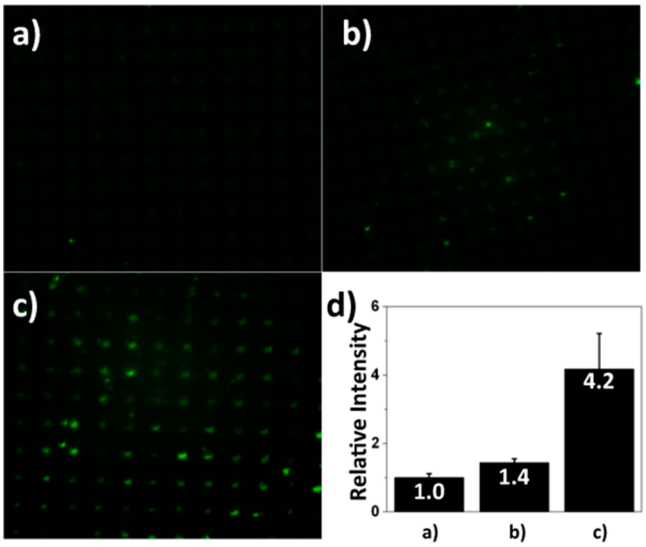

Figure 4. Comparing the different catalysts to promote hydrazone formation between hydrazide DNA labeled with FAM and exposed acetophenone (ketone) groups after photoillumination with (a) 10 mM aniline, (b) 10 mM anthranilic acid, and (c) 150 mM *m*-phenylenediamine in pH 4.5 buffer. (d) Densitometric data comparing the average fluorescence intensity per unit area on the pillars for the three different catalysts. The error bars represent standard deviations obtained from 10 pillars. The numbers are normalized to the intensity of the fluorescence obtained from using 10 mM aniline (a).

anthranilic acid is a very efficient reagent for catalyzing hydrazone formation at neutral pH, its solubility is limited in acidic buffer, which likely decreased the concentration of available catalyst. Control experiments confirmed that DNA was unable to attach to the surfaces in the absence of illumination (Figure 5), indicating that the reaction would proceed only in areas that displayed a ketone moiety. These experiments indicate that *m*-PDA is the most efficient catalyst for hydrazone formation between DNA hydrazides and surface-bound ketones, owing to its high solubility in acidic aqueous buffer.

Finally, we reasoned that by utilizing our photopatterning strategy, photoreactive carbonyls could be uncaged in a spatially controlled manner. Thus, it may be possible to attach different biomolecules to discrete regions of the same substrate. To study this, a 500 μm^2 mask was used to first reveal ketones in one region of a substrate; these photogenerated ketones were then reacted with FAM-conjugated hydrazide DNA. After DNA conjugation, the hydrazone bonds were reduced with $NaCNBH_3$ to form irreversible covalent bonds. Remaining ketone groups were blocked with PEG-hydrazine, and the remainder of the silicon surface, which was initially blocked by the mask, was exposed to light to reveal reactive ketone groups. These were then conjugated in a subsequent step with TAMRA-labeled hydrazine antigoat IgG. As shown in Figure 6, by using the photocaged ketone in conjunction with a mask,

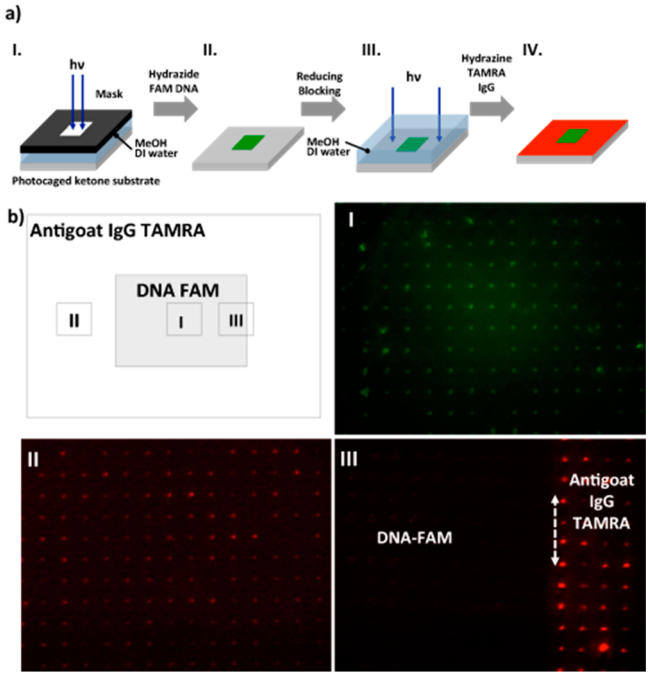

Figure 6. (a) Schematic showing methods used to pattern two types of biomolecules on the substrate via hydrazone chemistries. I. Light was first exposed through a mask in MeOH/H_2O. II. The photoexposed regions were next conjugated with FAM-labeled DNA. III. After reduction and PEG blocking, light was exposed in a second region of the sample. IV. These newly exposed regions were reacted with TAMRA-labeled hydrazine antigoat IgG. (b) Fluorescent images obtained. I. Fluoresent image of the DNA-FAM region. II. Fluorescent image of the TAMRA-antigoat IgG region. III. Fluorescent image showing the boundary region between DNA-FAM and TAMRA-antigoat IgG.

it was possible to pattern two different types of biomolecules on a single substrate with high bioconjugation yields and no cross reactivities.

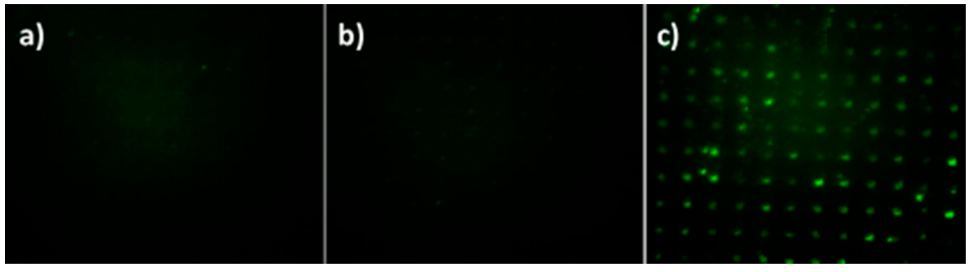

Figure 5. Conjugation of FAM-labeled hydrazide DNA to photopatterned surfaces. Fluorescent images of FAM-labeled hydrazide DNA on Si pillars. In all cases, 150 mM mPDA was used as a catalyst. (a) Fluorescent image showing no attachment of DNA to Si pillars displaying a photocaged ketone. (b) Fluorescent image showing no attachment of DNA to Si pillars after incubation in the photolysis buffer. (c) Fluorescence image showing DNA conjugated to the pillars after light exposure.

dx.doi.org/10.1021/la500744s | *Langmuir* 2014, 30, 8452−8460

CONCLUSIONS

We have demonstrated a facile and high-yield approach for covalently immobilizing DNA and proteins on photolithographically patterned silicon surfaces via hydrazone formation chemistry between surface-bound aldehydes with hydrazide- or hydrazine-derivatized biomolecules. DNA and proteins were successfully conjugated to aldehyde-modified silicon pillars in significantly higher yields than what could be achieved with maleimide−thiol coupling, a traditional bioconjugation methodology. Experiments with antibody−antigen pairs as well as enzymes demonstrate that the structural integrity of the proteins is preserved during and after conjugation to the surfaces. We have also designed and synthesized a molecule that can be anchored to a surface and prompted to reveal a hydrazine-reactive carbonyl in the presence of UV light. Time-course NMR studies establish that the compound undergoes clean photoconversion to its correspond acetophenone derivative. We demonstrate that this photorevealed ketone can be coupled to hydrazide/hydrazine nucleophiles in the presence of an *m*-PDA organocatalyst to achieve good coverage biomolecules in photopatterned areas. Finally, we highlight the ability of this approach for installing multiple biomolecules in discrete regions of the same substrate. We expect that this strategy will find applications in the develeopment of multiplexed assay production.

MATERIALS AND METHODS

Unless otherwise noted, all reagents were obtained from commercial sources and used without further purification. UV−vis spectra were acquired on a DU 730 spectrophotometer (Beckman Coulter, USA). ^{1}H and ^{13}C NMR spectra were recorded on 400 MHz NMR (Avance-III 400 NMR, Bruker). Photoirradiation experiments were carried out with a mercury lamp (200 W, X-cite exacte microscope illumination system, Lumen Dynamics, USA).

Photoresist-Capped Micrometer-Sized Silicon Pillar. Micropatterned silicon substrates were fabricated by reactive ion etching (RIE). Photoresist NR9-3000PY (Futurrex, Inc) was spun on the silicon wafer at 4000 rpm for 40 s to obtain a layer thickness of 2.5 μm. After a soft-bake step on a 150 °C hot plate for 60 s, the photoresist layer was exposed to 22 s of UV light in a MA6 mask aligner through a photomask (5 μm diameter and 10 μm spacing). Subsequently the wafer was baked on a 150 °C hot plate for 60 s (postexposure bake, PEB) and developed with an RD6 developer (Futurrex, Inc).

Poly(ethylene glycol) (PEG)-Passivated Amine-Modified Pillars. The above substrates were first treated with 2 M nitric acid for 1 h to hydroxylate the non-PR-coated areas. After being washed with DI water, the substrates were reacted with 5 mg/mL poly(ethylene glycol) (PEG)-silane (MW 5000) in toluene for 5 h and then washed with toluene, acetone (with sonication for 4.5 min for wahing and removing the photoresist), and ethanol. To form a covalent bond between the PEG chains and the Si surface, the substrates were next thermally treated at 120 °C for 30 min. The revealed Si pillar surfaces were hydroxylated with a 1 h, 2 M nitric acid treatment. The substrate was reacted with 5% v/v APTES ((3-aminopropyl)triethoxysilane) in ethanol overnight followed by heat treatment at 120 °C for 30 min to derivatize the pillars with amine groups.

DNA and Antibody Immobilized on the Aldehyde-Modified Pillars. The PEG-passivated amine-modified Si pillars were reacted with 4-formyl succinimidyl benzoate (200 μM) for 12 h in 100 mM $NaHCO_3$ buffer, pH 8.2, and then washed with 1× PBS (pH 7.2) buffer. The resulting aldehyde−silicon pillars were next reacted with 10 μM FAM-conjugated hydrazide A_{15} in 100 mM NH_4OAc buffer at pH 4.8 overnight, followed by washing with NH_4OAc buffer. To immobilize proteins, 1.5 mg/mL fluorescein-conjugated antigoat IgG was first reacted with 20 equiv of succinimidyl-6-hydrazinonicotinate acetone hydrazone (SANH, Solulink) for 3 h, followed by purification with a 7k MWCO spin desalting column (Thermo Scientific). Aldehyde−silicon pillars were then reacted with 2 μM hydrazine-fluorescein-conjugated antigoat IgG in 100 mM NH_4OAc buffer at pH 4.8 overnight, and the substrate was then washed with NH_4OAc buffer.

Alkaline Phosphatase Immobilized on the Aldehyde-Modified Pillars. Alkaline phosphatase (1 mg/mL) was first reacted with 20 equiv of SANH in MOPS buffer (pH 8.1, 100 mM MOPS, 150 mM NaCl, 2 mM $MgCl_2$, 0.1 mM $ZnCl_2$) for 2.5 h, followed by purification with a 7k MWCO spin desalting column (Thermo Scientific). Aldehyde−silicon pillars were then reacted with 2 μM hydrazine-conjugated alkaline phosphatase in 100 mM NH_4OAc, 150 mM NaCl, 3 mM $MgCl_2$ buffer at pH 4.8 overnight followed by washing with NH_4OAc buffer. The resulting alkaline phosphatase-covered silicon pillars were incubated with fluorogenic phosphatase substrate ELF-97 (20 μM) (Molecular Probes, OR) in glycine buffer (100 mM, 1 mM $MgCl_2$, 1 mM $ZnCl_2$) at pH 10.

Synthesis of a Photocaged Ketone Compound. The synthesis route to photoactivate ketone compound **2** is shown in Scheme 1. Detailed synthesis procedures and NMR spectra are provided as follows.

*4-Ethyl-3-nitrobenzoic Acid (**3**).* A 50 mL round-bottomed flask was immersed in a water bath at room temperature, and concentrated sulfuric acid (5 mL) was carefully added to concentrated nitric acid (60−70%, 5 mL). 4-Ethylbenzoic acid (1.00 g, 6.6 mmol) was added in a single portion. The flask was capped with a septum, and a precipitate formed after ca. 60 s. The reaction was allowed to proceed for 3 h at room temperature, at which point it was poured into a beaker with ice. The reaction was filtered, and the white solid was washed with water, collected, and dried (1.26 g, 97%). ^{1}H NMR (400 MHz, DMSO-d_6) δ 8.34 (d, J = 1.8 Hz, 1H), 8.13 (dd, J = 8.0, 1.8 Hz, 1H), 7.65 (d, J = 8.1 Hz, 1H), 2.87 (q, J = 7.5 Hz, 2H), 1.22 (t, J = 7.5 Hz, 3H).

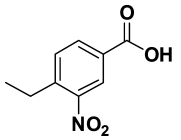

*Methyl-4-ethyl-3-nitrobenzoate (**4**).* A 20 mL scintillation vial was charged with a stirbar, **2** (390 mg, 2.0 mmol), EDC (465 mg, 3.0 mmol, 1.5 equiv), *N*-hydroxysuccinimide (277 mg, 2.4 mmol, 1.2 equiv), and CH_2Cl_2 (10 mL). The reaction was allowed to proceed at room temperature for 6 h, at which point it was washed with water (2× 5 mL) and brine (1× 5 mL) and dried over $MgSO_4$. The solvent was removed by rotary evaporation to yield a light-yellow oil that crystallized into lemon-yellow crystals upon standing. The crude material was dissolved in MeOH (25 mL), and NaOMe (5.4 M solution in MeOH) was added (840 uL, 2.0 equiv). The reaction was monitored by TLC (CH_2Cl_2), and after 30 min, the reaction was diluted with EtOAc (5 mL) and CH_2Cl_2 (20 mL) and washed with water (2× 10 mL), and the organic phase was dried over $MgSO_4$. Concentration in vacuo provided pale-yellow oil (332 mg, 79% over two steps). ^{1}H NMR (400 MHz, $CDCl_3$) δ 8.54 (d, J = 1.8, 1H), 8.19 (dd, J = 8.0, 1.8 Hz, 1H), 7.49 (d, J = 8.1, 1H), 3.98 (s, 3H), 2.97 (q, J = 7.5 Hz, 2H), 1.33 (t, J = 7.5 Hz, 3H).

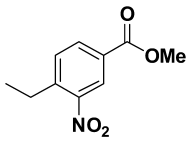

*Methyl 4-(1-bromoethyl)-3-nitrobenzoate (**5**).* *N*-Bromosuccinimide (309 mg, 1.75 mmol) and benzoyl peroxide (30 mg) were added to a benzene solution (10 mL) of **3** (242 mg, 1.16 mmol). The reaction was brought to reflux for 14 h in the dark, at which point it was cooled to room temperature and the organic phase was washed with water (2× 10 mL) and brine (1× 10 mL). The organic phase was separated and dried over $MgSO_4$. Concentration in vacuo furnished a dark-orange oil. This compound coeluted with the only major impurity, so the crude material was subjected to the next reaction

dx.doi.org/10.1021/la500744s | *Langmuir* 2014, 30, 8452−8460

without any further purification. ^{1}H NMR indicated that the material is ca. 75% pure. ^{1}H NMR (400 MHz, $CDCl_3$) δ 8.50 (d, J = 1.8, 1H), 8.29 (dd, J = 8.0, 1.8 Hz, 1H), 8.00 (d, J = 8.3, 1H), 5.82 (q, J = 6.8 Hz, 1H), 4.00 (s, 3H), 2.12 (d, J = 6.8 Hz, 3H).

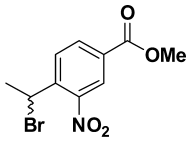

*Methyl 4-(1-Methoxyethyl)-3-nitrobenzoate (**6**).* A 20 mL scintillation vial was charged with a stirbar, **4** (100 mg, 0.48 mmol), $AgNO_3$ (100 mg, 0.6 mmol), and MeOH (5 mL). The vial was protected from light, and the reaction was stirred overnight at room temperature. The precipitated AgBr was filtered off, and the filtrate was concentrated. ^{1}H NMR (400 MHz, $CDCl_3$) δ 8.60 (dd, J = 1.7, 0.4 Hz, 1H), 8.31 (dd, J = 8.2, 1.7 Hz, 1H), 7.88 (d, J = 8.2 Hz, 1H), 4.98–4.91 (m, 1H), 4.00 (s, 3H), 3.25 (s, 3H), 1.55 (d, J = 6.3 Hz, 3H).

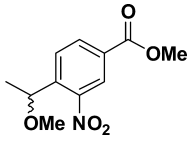

*4-(1-Methoxyethyl)-3-nitrobenzoic Acid (**7**).* A 4 mL vial was charged with a stirbar, **5** (10 mg, 0.04 mmol), LiCl (8.8 mg, 0.2 mmol), NaOH (8.4 mg, 0.2 mmol), and 95% MeOH (3 mL). The reaction was stirred in the dark at room temperature for 3 h, at which point the solution was concentrated, diluted with H_2O (5 mL), and neutralized with HCl (2.5 M). The aqueous phase was extracted with CH_2Cl_2 (2× 5 mL), and the organic phase was dried over $MgSO_4$. Filtration and concentration provided **6** as a light-brown solid (9 mg, 98%). The residue was dissolved in ethyl acetate, and petroleum ether slowly diffused into it to provide **6** as a white solid. ^{1}H NMR (400 MHz, $CDCl_3$) δ 8.66 (s, 1H), 8.37 (d, J = 8.2, 1H), 7.91 (d, J = 8.2 Hz, 1H), 4.96 (q, J = 6.3 Hz, 1H), 3.26 (s, 3H), 1.56 (d, J = 6.3 Hz, 3H).

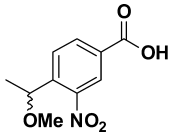

*2,5-Dioxopyrolidin-1-yl 4-(1-methoxy-ethyl)-3-nitro-benzoate (**2**).* A 20 mL scintillation vial was charged with a stirbar, **6** (9 mg, 0.04 mmol), EDC (12.4 mg, 0.08 mmol), NHS (6.9 mg, 0.06 mmol), and CH_2Cl_2 (2 mL). The reaction was protected from light, and the solution was stirred at room temperature for 5 h. The reaction was diluted with H_2O (3 mL) and CH_2Cl_2 (5 mL), and the layers were separated. The organic phase was washed with H_2O (1× 2 mL) and brine (1× 2 mL), and the organic phase was dried over $MgSO_4$. The reaction was concentrated by rotary evaporation to give a light-yellow oil. ^{1}H NMR (400 MHz, $CDCl_3$) δ 8.72 (dd, J = 1.8, 0.4 Hz, 1H), 8.41 (dd, J = 8.2, 1.8 Hz, 1H), 7.99 (dt, J = 8.3, 0.5 Hz, 1H), 5.03–4.94 (m, 1H), 3.27 (s, 3H), 2.96 (s, 4H), 1.56 (d, J = 6.3 Hz, 3H).

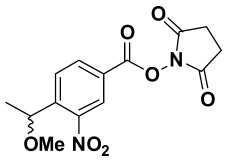

Photolysis of 1 and 7 by UV Irradiation. Seven milligrams of **1** and **7** was dissolved in 500 μL of MeOH/DI water (3:1). Solutions containing the photocaged carbonyl compounds were transferred to NMR tubes and illuminated with a UV light source (200 W, mercury lamp) (Figures 2 and S4). After different amounts of irradiation, the degree of photolysis (**1** to **1′**, **7** to **7′**) was monitored by ^{1}H NMR.

DNA and Antibody Immobilized on the Photocaged Ketone-Modified Pillars. The amine-modified Si pillars were reacted with 10 mM NHS-ester **2** for 12 h in 1 mL of CH_2Cl_2/Me_2SO (9:1) and then washed with CH_2Cl_2. The photocaged ketone–silicon pillars were next irradiated with UV light for 30 min and then incubated in pH 8.0 10 mM phosphate buffer. The photolyzed ketone–Si pillars were then reacted with 25 μM of FAM-conjugated hydrazide-DNA at pH 4.5 and in the presence of 150 mM *m*-phenylenediamine (*m*-PDA) overnight. The formed hydrazones between the photolyzed ketone and FAM-modified hydrazide DNA were reduced with 5 mM $NaCNBH_3$ at pH 4.0 to form irreversible covalent bonds. Any remaining unreacted ketones were reacted with 1 M hydrazide PEG and 150 mM *m*-PDA at pH 4.5. For the DNA and protein arrays, the DNA patterns were generated following the aforementioned steps. Next, the rest of the surface was illuminated to expose ketone groups which were then reacted with 2 μM TAMRA-conjugated hydrazine antigoat IgG in 150 mM *m*-PDA at pH 4.5.

■ ASSOCIATED CONTENT

Supporting Information

Fluorescent images of fluorescein-labeled antigoat IgG reacted silicon pillars, fluorescein-labeled goat IgG reacted antigoat IgG immobilized silicon pillars, and alkaline phosphatase immobilized silicon pillars. Photolysis to produce active aldehydes upon photoillumination and ^{1}H NMR spectra monitoring the photoconversion of **1**. Amine-modified pillars reacted with the NHS-ester of 4-carboxyacetophenone (NHS-acetophenone) to install acetophenone (ketone) moieties on the pillars. Photolysis to produce active ketones upon photoillumination. Comparison of fluorescence intensity line plots obtained with ImageJ. This material is available free of charge via the Internet at http://pubs.acs.org.

■ AUTHOR INFORMATION

Corresponding Author

*E-mail: Jennifer.Cha@colorado.edu.

Author Contributions

J.H.L. and D.W.D. contributed equally to this work.

Notes

The authors declare no competing financial interest.

■ ACKNOWLEDGMENTS

This work was supported by an NSF Career Award (DMR-1056808), the Office of Naval Research (award no. N00014-09-01-0258), and a DOE Early Career Award (DE-SC0006398). H.N. was supported by DOE DE-SC0006398. We thank Prof. Andrew Goodwin for help in editing the article.

■ REFERENCES

(1) Hoopes, L. Genetic Diagnosis: DNA Microarrays and Cancer. *Nat. Educ.* **2008**, *1*, 1.

(2) DeRisi, J.; Penland, L.; Brown, P. O.; Bittner, M. L.; Meltzer, P. S.; Ray, M.; Chen, Y.; Su, Y. A.; Trent, J. M. Use of a cDNA Microarray to Analyse Gene Expression Patterns in Human Cancer. *Nat. Genet.* **1996**, *14*, 457–460.

(3) Schena, M.; Shalon, D.; Davis, R. W.; Brown, P. O. Quantitative Monitoring of Gene Expression Patterns with A Complementary DNA Microarray. *Science* **1995**, *270*, 467–470.

(4) Lockhart, D. J.; Winzeler, E. A. Genomics, Gene Expression and DNA Arrays. *Nature* **2000**, *405*, 827–836.

(5) Eisen, M. B.; Spellman, P. T.; Brown, P. O.; Botstein, D. Cluster Analysis and Display of Genome-Wide Expression Patterns. *Proc. Natl. Acad. Sci. U.S.A.* **1998**, *95*, 14863–14868.

(6) Zhang, S.; Yan, L.; Altman, M.; Lässle, M.; Nugent, H.; Frankel, F.; Lauffenburger, D. A.; Whitesides, G. M.; Rich, A. Biological Surface Engineering: A Simple System for Cell Pattern Formation. *Biomaterials* **1999**, *20*, 1213–1220.

(7) MacBeath, G.; Schreiber, S. L. Printing Proteins as Microarrays for High-Throughput Function Determination. *Science* **2000**, *289*, 1760–1763.

(8) Zhu, H.; Bilgin, M.; Bangham, R.; Hall, D.; Casamayer, A.; Bertone, P.; Lan, N.; Jansen, R.; Bidlingmaier, S.; Houfek, T.; Mitchell, T.; Miller, P.; Dean, R. A.; Gerstein, M.; Snyder, M. Global Analysis of Protein Activities Using Proteome Chips. *Science* **2001**, *293*, 2101−2105.
(9) Christman, K. L.; Requa, M. V.; Enriquez-Rios, V. D.; Ward, S. C.; Bradley, K. A.; Turner, K. L.; Maynard, H. D. Submicron Streptavidin Patterns for Protein Assembly. *Langmuir* **2006**, *22*, 7444−7450.
(10) Kannan, B.; Castelino, K.; Chen, F. F.; Majumdar, A. Lithographic Techniques and Surface Chemistries for the Fabrication of PEG-Passivated Protein Microarrays. *Biosens. Bioelectron.* **2006**, *21*, 1960−1967.
(11) Bailey, R. C.; Kwong, G. A.; Radu, C. G.; Witte, O. N.; Heath, J. R. DNA-Encoded Antibody Libraries: A Unified Platform for Multiplexed Cell Sorting and Detection of Genes and Proteins. *J. Am. Chem. Soc.* **2007**, *129*, 1959−1967.
(12) Kim, J.; Cho, J.; Seidler, P. M.; Kurland, N. E.; Yadavalli, V. K. Investigations of Chemical Modifications of Amino-Terminated Organic Films on Silicon Substrates and Controlled Protein Immobilization. *Langmuir* **2010**, *26*, 2599−2608.
(13) Zhang, C.-J.; Tan, C. Y. J.; Ge, J.; Na, Z.; Chen, G. Y. J.; Uttamchandani, M.; Sun, H.; Yao, S. Q. Preparation of Small-Molecule Microarrays by trans-Cyclooctene Tetrazine Ligation and Their Application in the High-Throughput Screening of Protein−Protein Interaction Inhibitors of Bromodomains. *Angew. Chem., Int. Ed.* **2013**, *52*, 14060−14064.
(14) Doh, J.; Irvine, D. J. Immunological Synapse Arrays: Patterned Protein Surfaces That Modulate Immunological Synapse Structure Formation in T Cells. *Proc. Natl. Acad. Sci. U.S.A.* **2006**, *103*, 5700−5705.
(15) Wilson, D. S.; Nock, S. Recent Developments in Protein Microarray Technology. *Angew. Chem., Int. Ed.* **2003**, *42*, 494−500.
(16) Langer, R.; Tirrell, D. A. Designing Materials for Biology and Medicine. *Nature* **2004**, *428*, 487−492.
(17) Kingsmore, S. F. Multiplexed Protein Measurement: Technologies and Applications of Protein and Antibody Arrays. *Nat. Rev. Drug Discovery* **2006**, *5*, 1474−1776.
(18) Robinson, W. H.; Digennaro, C.; Hueber, W.; Haab, B. B.; Kamachi, M.; Dean, E.; Fournel, S.; Fong, D.; Genovese, M. C.; Neuman De Begvar, H. E.; Skriner, K.; Hirschberg, D. L.; Morris, R. I.; Muller, S.; Prujin, G. J.; Van Verooij, W. J.; Smolen, J.S.; Brown, P. O.; Steinman, L.; Utz, P. J. Antiantigen Microarrays for Multiplex Chracterization of Autoantibody Responses. *Nat. Med.* **2002**, *8*, 295−301.
(19) Schweitzer, B.; Roberts, S.; Grimwade, B.; Shao, W.; Wang, M.; Fu, Q.; Shu, Q.; Laroche, L.; Zhou, Z.; Tchernev, V. T.; Christiansen, J.; Velleca, M.; Kingsmore, S. F. Mutiplexed Protein Profiling on Microarrays by Rolling-Circle Amplification. *Nat. Biotechnol.* **2002**, *20*, 359−365.
(20) Angenendt, P.; Gölkler, J. r.; Sobek, J.; Lehrach, H.; Cahill, D. J. Next Generation of Protein Microarray Support Materials: Evaluation for Protein and Antibody Microarray Applications. *J. Chromatogr., A* **2003**, *1009*, 97−104.
(21) Kusnezow, W.; Jacob, A.; Walijew, A.; Diehl, F.; Hoheisel, J. D. Antibody Microarrays: An Evaluation of Production Parameters. *Proteomics* **2003**, *3*, 254−264.
(22) Kimura, N.; Oda, R.; Inaki, Y.; Suzuki, O. Attachment of Oligonucleotide Probes to Poly Carbodiimide-coated Glass for Microarray Applications. *Nucleic Acids Res.* **2004**, *32*, e68.
(23) Rozsnyai, L. F.; Benson, D. R.; Fodor, S. P.; Schultz, P. G. Photolithographic Immobilization of Biopolymers on Solid Supports. *Angew. Chem., Int. Ed.* **1992**, *31*, 759−761.
(24) Herbert, C. B.; McLernon, T. L.; Hypolitel, C. L.; Adams, D. N.; Pikusl, L.; Huang, C.-C.; Fields, G. B.; Letourneau, P. C.; Distefano, M. D.; Hu, W. S. Micropatterning Gradients and Controlling Surface Densities of Photoactivatable Biomolecules on Self-assembled Monolayers of Oligo(ethylene glycol) Alkanethiolates. *Chem. Biol.* **1997**, *4*, 731−737.
(25) Toh, C. R.; Fraterman, T. A.; Walker, D. A.; Bailey, R. C. Direct Biophotolithographic Method for Generating Substrates with Multiple Overlapping Biomolecular Patterns and Gradients. *Langmuir* **2009**, *25*, 8894−8898.
(26) Martin, T. A.; Herman, C. T.; Limpoco, F. T.; Michael, M. C.; Potts, G. K.; Bailey, R. C. Quantitative Photochemical Immobilization of Biomolecules on Planar and Corrugated Substrates: A Versatile Strategy for Creating Functional Biointerfaces. *ACS Appl. Mater. Interfaces* **2011**, *3*, 3762−3771.
(27) Angenendt, P. Progress in Protein and Antibody Microarray Technology. *Drug Discovery Today* **2005**, *10*, 503−511.
(28) O'Donovan, L.; De Bank, P. A. A Photocleavable Linker for the Chemoselective Functionalization of Biomaterials. *J. Mater. Chem.* **2012**, *22*, 21878−21884.
(29) Dirksen, A.; Dirksen, S.; Hackeng, T. M.; Dawson, P. E. Nucleophilic Catalysis of Hydrazone Formation and Transimination: Implications for Dynamic Covalent Chemistry. *J. Am. Chem. Soc.* **2006**, *128*, 15602−15603.
(30) Dirksen, A.; Hackeng, T. M.; Dawson, P. E. Nucleophilic Catalysis of Oxime Ligation. *Angew. Chem., Int. Ed.* **2006**, *45*, 7581−7584.
(31) Kalia, J.; Raines, R. T. Hydrolytic Stability of Hydrazones and Oximes. *Angew. Chem., Int. Ed.* **2008**, *47*, 7523−7526.
(32) Dirksen, A.; Dawson, P. E. Rapid Oxime and Hydrazone Ligations with Aromatic Aldehydes for Biomolecular Labeling. *Bioconjugate Chem.* **2008**, *19*, 2543−2548.
(33) Domaille, D. W.; Lee, J. H.; Cha, J. N. High Density DNA Loading on the M13 Bacteriophage Provides Access to Colorimetric and Fluorescent Protein Microarray Biosensors. *Chem. Commun.* **2013**, *49*, 1759−1761.
(34) Byeon, J.-Y.; Limpoco, F. T.; Bailey, R. C. Efficient Bioconjugation of Protein Capture Agents to Biosensor Surfaces Using Aniline-Catalyzed Hydrazone Ligation. *Langmuir* **2010**, *26*, 15430−15435.
(35) Lee, J. H.; Xu, P. F.; Domaille, D. W.; Choi, C.; Jin, S.; Cha, J. N. M13 Bacteriophage as Materials for Amplified Surface Enhanced Raman Scattering Protein Sensing. *Adv. Funct. Mater.* **2014**, *24*, 2079−2084.
(36) McKinnon, D. D.; Domaille, D. W.; Cha, N. J.; Anseth, K. S. Biophysically Defined and Cytocompatible Covalently Adaptable Networks as Viscoelastic 3D Cell Culture Systems. *Adv. Mater.* **2014**, *26*, 865−872.
(37) Kool, E. T.; Park, D.; Pete Crisalli, P. Fast Hydrazone Reactants: Electronic and Acid/Base Effects Strongly Influence Rate at Biological pH. *J. Am. Chem. Soc.* **2013**, *135*, 17663−17666.
(38) Zhu, Y.; Gupta, B.; Guan, B.; Ciampi, S.; Reece, P. J.; Gooding, J. J. Photolithographic Strategy for Patterning Preformed, Chemically Modified, Porous Silicon Photonic Crystal Using Click Chemistry. *ACS Appl. Mater. Interfaces* **2013**, *5*, 6514−6521.
(39) Bernard, A.; Renault, J. P.; Michel, B.; Bosshard, H. R.; Delamarche, E. Microcontact Printing of Proteins. *Adv. Mater.* **2000**, *12*, 1067−1070.
(40) Bernard, A.; Fitzli, D.; Sonderegger, P.; Delamarche, E.; Michel, B.; Bosshard, H. R.; Biebuyck, H. Affinity Capture of Proteins from Solution and Their Dissociation by Contacting Printing. *Nat. Biotechnol.* **2001**, *19*, 866−869.
(41) Corrie, J. E. T.; Barth, A.; Munasinghe, V. R. N.; Trentham, D. R.; Hutter, M. C. Photolytic Cleavage of 1-(2-Nitrophenyl)ethyl Ethers Involves Two Parallel Pathways and Product Release Is Rate-Limited by Decomposition of A Common Hemiacetal Intermediate. *J. Am. Chem. Soc.* **2003**, *125*, 8546−8554.
(42) Il'ichev, Y. V.; Schwörer, M. A.; Wirz, J. Photochemical Reaction Mechanisms of 2-Nitrobenzyl Compounds: Methyl Ethers and Caged ATP. *J. Am. Chem. Soc.* **2004**, *126*, 4581−4595.
(43) Yang, Y.; Shao, Q.; Deng, R.; Wang, C.; Teng, X.; Cheng, K.; Cheng, Z.; Huang, L.; Liu, Z.; Liu, X.; Xing, B. In Vitro and In Vivo Uncaging and Bioluminescence Imaging by Using Photocaged Upconversion Nanoparticles. *Angew. Chem., Int. Ed.* **2012**, *51*, 3125−3129.

(44) Klein, D. *Organic Chemistry*, 2nd ed.; John Wiley and Sons: Hoboken, N.J., 2011.
(45) Rashidian, M.; Mahmoodi, M. M.; Shah, R.; Dozier, J. K.; Wagner, C. R.; Distefano, M. D. A. Highly Efficient Catalyst for Oxime Ligation and Hydrazone-Oxime Exchange Suitable for Bioconjugation. *Bioconjugate Chem.* **2013**, *24*, 333−342.
(46) Crisalli, P.; Kool, E. T. Water-Soluble Organocatalysts for Hydrazone and Oxime Formation. *J. Org. Chem.* **2013**, *78*, 1184−1189.

dx.doi.org/10.1021/la500744s | *Langmuir* 2014, 30, 8452−8460